

# Building a computational model of active deformable particles

Eden-Rae Wedderburn<sup>1,\*</sup> and Luke K. Davis<sup>2,†</sup>

<sup>1</sup>*Department of Physics and Astronomy, University College London, 25 Gordon Street, London, England*

<sup>2</sup>*Department of Mathematics, University College London, 25 Gordon Street, London, England*

Deformable cells are ubiquitous in living systems and often form the fundamental microscopic unit to which interesting collective behaviour emerges. Typically, these cells are out-of-equilibrium, due to the burning of fuel to sustain cellular motion and/or shape shifting, and thus respond to various external stimuli and environments in a way that cannot be wholly captured using standard equilibrium physics. Moreover, a unifying picture of how deformable cells behave in different circumstances is currently lacking. Here, we build a rather simple active deformable particle model, that retains the complexity of non-isotropic deformation degrees of freedom yet allows for the efficient exploration of the roles of active forces. In so doing we propose a novel way of implementing active bonds and investigate how such forces govern the dynamics and morphology of the deformable cell. Overall, we present a highly flexible model that can be used as a basis to unify seemingly disparate experimental observations on biological cells.

## I. INTRODUCTION

How do biological cells move and behave as a function of their environment? This question might harken back to 1655 when Robert Hooke first discovered the cell. Currently, this question is at the heart of a wide-range of biological and biophysical research. As physicists, understanding how biological cells behave is made difficult by two facts: (i) biological cells are intrinsically out-of-equilibrium, and (ii) they exhibit degrees of freedom not typical of previously studied physical systems. For example, in animal (eukaryotic) cells, movement can be accomplished through cell-protrusions (or Filopodia) through a sequence of protrusion, attachment, and retraction [1, 2]. The out-of-equilibrium nature of biological cells means that we cannot blindly use physical models and theories that rest on thermal equilibrium assumptions. Indeed, this is the challenge facing and being addressed by the field of active matter: systems whose constituents burn fuel that drive collective behaviour not seen at thermal equilibrium [3, 4].

There is, now, a large body of experimental observations concerning many types of deformable biological cells ranging from dense packings of oligodendroglia cells to in-vitro cell migration experiments. These observations are sometimes supplemented with bespoke physical models that include particle (or agent) based models, continuum models, vertex and other modelling approaches. Despite the progress in modelling specific experimental settings, a wide-reaching, unifying, model that can (at least qualitatively) explain seemingly disparate experimental observations is currently missing.

Here, we build a rather minimal – “fried-egg” – active deformable particle model that is able to capture, per-cell, non-isotropic (deformable) degrees of freedom and where one can directly explore the roles of internal active

forces (see Figure 2D). To probe possible mechanisms of cell response and movement we here explore the roles of self-propulsion of the central and necklace beads and, separately, active internal and necklace bonds.

The paper is structured as follows: in section II we present the theoretical and computational underpinnings of the model, then, in section III we show the results for passive and active deformable particles, and, finally, in section IV we summarise and discuss our findings.

## II. APPROACH

To construct our model of a deformable particle, we will combine our original equation-based theory with computer simulations.

In the model, there will be a necklace of beads along

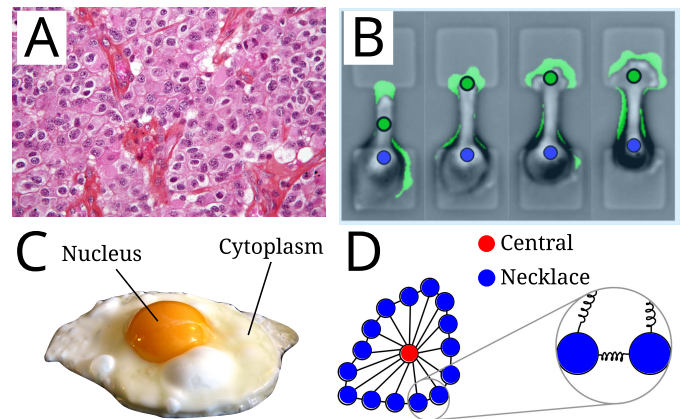


FIG. 1. **A** High magnification micro-graph of an oligodendroglia, where “fried-egg”-like cells have a clear cytoplasm and well-define borders. **B** Cell-migration in a confined, dumbbell-like, geometry where the nucleus and protrusion are highlighted in blue and green respectively (taken from [5]). **C** A fried-egg. **D** Basic ingredients of our deformable particle model.

\* eden-rae.wedderburn.21@ucl.ac.uk

† luke.davis@ucl.ac.uk

the exterior joined by bonds modelled as classical springs. There will also be a central bead that orchestrates the motion of the springs and therefore over the particle as a whole, as seen in the Figure 2D.

The springs connecting the outer ‘necklace’ beads all

$$H = \underbrace{\frac{1}{2}m \left( \sum_{i=1}^N (\dot{\vec{r}}_i)^2 \right)}_{\text{Kinetic Energy}} + \underbrace{\frac{1}{2}k_n \left( \sum_{i=2}^N (r_{i,i+1} - l_n)^2 + (r_{N,2} - l_n)^2 \right)}_{\text{Potential of Necklace Bonds}} + \underbrace{\frac{1}{2} \sum_{i=2}^N k_i (|\vec{r}_1 - \vec{r}_i| - l)^2}_{\text{Potential of Internal Bonds}} + \underbrace{\frac{1}{2} \sum_{i,j}^N V(|r_i - r_j|)}_{\text{Interaction Potential}}, \quad (1)$$

where  $N$  is the total number of beads,  $r_{i,j}$  is the distance between bead  $i$  and bead  $j$ ,  $k_n$  is the spring constant for each of the necklace bonds,  $l_n$  is the resting necklace bond length,  $k_i$  is the spring constant for the internal bonds, and  $V(|r_i - r_j|)$  is the interaction potential.

### A. Passive deformable particle model

The dynamics (equation of motion) of this system is given by:

$$\dot{\vec{r}}_i = -\mu \vec{\nabla}_i U(\{\vec{r}\}) + \sqrt{2D} \vec{\eta}_i, \quad (2)$$

where  $\mu$  is the mobility coefficient,  $\vec{\nabla}_i U$  is the gradient of the potential energy with respect to the particles position,  $D$  is the diffusion coefficient, and  $\vec{\eta}_i$  is a random variable.

### B. Active deformable particle model

The most straightforward way of making the above passive model active is by adding an additional term to the equation of motion (2) that represents an active self-propulsion,  $\vec{v}_i$  [4].

$$\dot{\vec{r}}_i = -\mu \vec{\nabla}_i U(\{\vec{r}\}) + \sqrt{2D} \vec{\eta}_i + \vec{v}_i. \quad (3)$$

As  $\vec{r}_i$  represents the derivative of the position vector of bead  $i$ , this equation can be applied in two ways: (i) bead  $i$  corresponds to the central bead or (ii) bead  $i$  corresponds to a necklace bead. This implies, activity can be present in any bead individually or in various combinations.

### C. Simulation details

When computationally modelling the system, each bead must have an initial position. For the simplest scenario (where the separation between beads are equal to the natural length of the springs between them  $r = l$ ),

have the same spring constant,  $k_n$ . However, the internal bonds or ‘springs’ have differing spring constants. Currently  $k_n$  is a constant rather than a function of time.

The total energy of the system (or the Hamiltonian) is the sum of kinetic  $T$  and potential energies  $U$  ( $H = T + U$ ) and, for this passive system, it is given as follows:

the potential energy for the necklace and internal bonds will be zero. As all of the internal bonds are equivalent and all of the necklace bonds are equivalent, the shape of the particle in this scenario is an equilateral polygon. Using polar co-ordinates, the initial positions for each of the beads in this simple scenario will be separated by  $2\pi/N$  where  $N$  is the total number of particles.

$$x = l \cos\left(\frac{2\pi}{N}\right), \quad y = l \sin\left(\frac{2\pi}{N}\right), \quad (4)$$

As we are working in 2D,  $z=0$ .

For our simulation, the interaction potential,  $V(|r_i - r_j|)$ , referred to in our Hamiltonian (1) will be given using the Weeks-Chandler-Andersen model seen below,

$$V_{\text{WCA}}(r_{ij}) = \begin{cases} 4\epsilon \left[ \left( \frac{\sigma_{ij}}{r_{ij}} \right)^{12} - \left( \frac{\sigma_{ij}}{r_{ij}} \right)^6 + \frac{1}{4} \right] & \text{if } r \leq 2^{1/6} \sigma_{ij} \\ 0 & \text{if } r > 2^{1/6} \sigma_{ij}, \end{cases} \quad (5)$$

where  $\sigma_{ij} = (d_i + d_j)/2$  is the closest approach distance between two beads.

For the initial configuration of the deformable particle,  $l$  can be determined using the following equation:

$$l = \begin{cases} \frac{(N-1) \cdot d_n}{2\pi} & \text{when } N \geq 8 \\ \frac{(8-1) \cdot d_n}{2\pi} & \text{when } N < 8. \end{cases} \quad (6)$$

where  $d_n$  is the diameter of the necklace particles. This represents the configuration in which the necklace particles are most closely packed together without overlapping. This is calculated by considering the distanced between two, adjacent necklace particles,  $l_n$ . The perimeter of the polygon that these necklace bonds produce is equivalent to the length of one bond, multiplies by the number of bonds in the necklace,  $l_n \cdot (N-1)$ . Considering that the most closely packed the necklace beads could be is the distance of one of their diameters,  $l_n = d_n$ . Modelling the necklace as a circle means that  $2\pi l = (N-1) \cdot d_n$  and rearranging gives the equation as seen before, (6).

Note that for  $N < 8$ , equation(6) fails as necklace beads overlap with the central internal bead due to geometric constraints of nearest neighbour packing. As the configuration we want can't be achieved in this model, for  $N < 8$ ,  $l$  is calculated using  $N = 8$ .

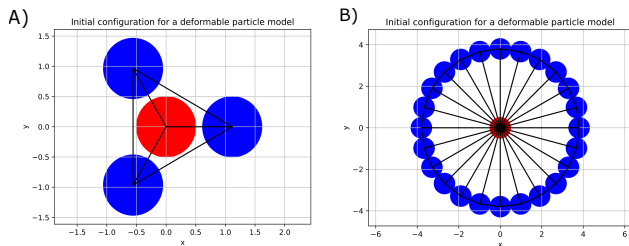


FIG. 2. Model of particle configuration for  $N=4$  (A) and  $N=25$  (B)

After producing an infile for LAMMPS to run, and animating the returned positions using matplotlib, an initial simulation of a passive deformable particle is produced.

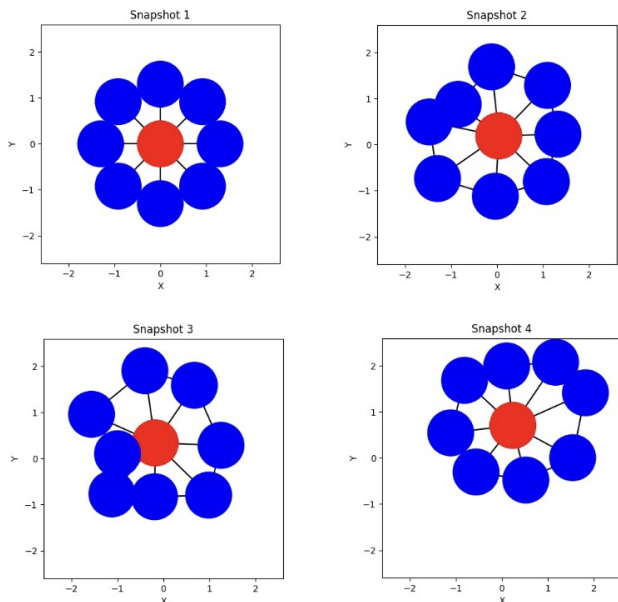


FIG. 3. Equally spaced snapshots of the animation for  $N = 9$ .

Further animation with different values of  $N$  led us to a value that will be used in subsequent modelling,  $N = 200$ . A larger value of  $N$  more closely mimics a solid surface or membrane. The diameter of the central (red) bead also should be increased, this produced the final "fried-egg" deformable particle model. Bonds have now been removed for visualisation purposes.

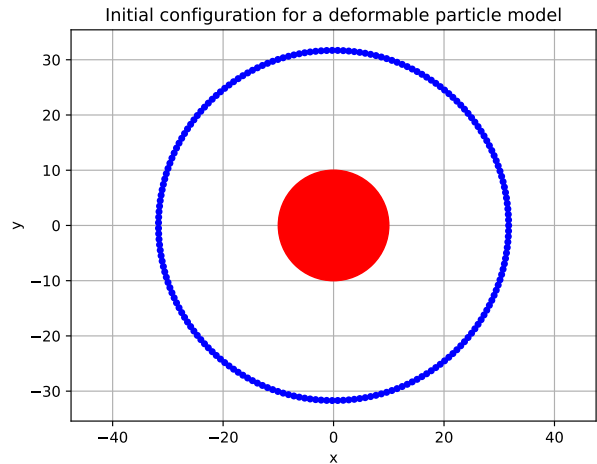


FIG. 4. "Fried-egg" initial configuration for  $N = 200$ .

### III. RESULTS

#### A. Validating simulation code

I validated the initialisation code by successfully producing numerous initial configurations of deformable particles with  $N$  values ranging between  $N = 4$  and  $N = 500$ , examples are shown in 2. The python code used to generate the initial configuration styles, is only limited by the computer running the code.

I validated the molecular dynamics algorithm (LAMMPS) code by successfully running numerous passive deformable particles as seen in 3. For the case  $N = 9$ , this figure accurately demonstrates the elasticity of the bonds and presence of interaction potential as beads are not overlapping.

#### B. Passive case

The spring constant of each of the bonds was initially 1. In 5 we begin to explore the effects of changing the spring constant of the internal and necklace bonds. The particles with higher spring constants have a more rigid shape (comparable to the initial configuration) whereas smaller spring constants have a more flexible necklace, barely resembling a membrane. To model using the parameters to the right hand side of the phase diagram would be inadvisable. These systems lose the characteristic of being deformable and would conclude the investigation prematurely. Like wise, the bottom left hand corner represents models that don't have a solid and stable membrane. Parameters  $k = 0.01$  and  $k_n = 1$  are most ideal to pursue with as the model produced most accurately mirrors a cell.

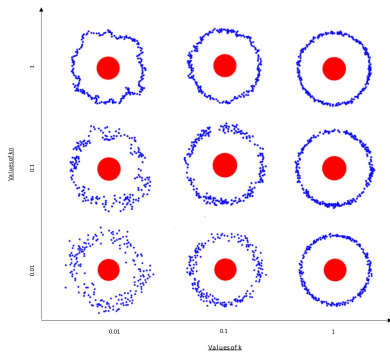


FIG. 5. Deformable particles where spring constant for bonds in the necklace ( $kn$ ) and internal bonds ( $k$ ) differ

### C. Active Case

In this section we will develop a new way of implementing active bonds. This is done by applying a force on each bead ( $i$  and  $j$ ) on either side of a bond to induce extension and contraction.

$$\vec{f}_i = f(-1)^{\gamma_{ij}} \hat{l}_{ij}, \quad (7)$$

$$\vec{f}_j = -\vec{f}_i. \quad (8)$$

$\vec{f}_i$  represents the force on bead  $i$  and  $\vec{f}_j$  on bead  $j$ .  $\gamma_{ij}$  is used as a switch to fluctuate between 1 (odd) or 2 (even), which allows for the forces to change between being positive and negative which concludes extension or contraction of the bond.  $\hat{l}_{ij}$  is the unit vector along

the bond. The direction of the unit vector is determined by the vector difference of the position of bead  $i$  and  $j$ .

LAMMPS currently does not support this active bond model despite its simplicity in principle. Consequently, we have built python code that integrates with LAMMPS but allows for the manipulation of each of the particles forces, allowing for us to simulate active bonds.

## IV. OUTCOMES

In summary, we have built an minimal, easily scaleable active deformable model. Our exploration of the passive case has given us insights into the appropriate ranges of key parameters in the model and visual confirmation of non-active behaviours. Governing equations on the theory to implement activity have been written and a new and simple way of creating active bonds has been produced. Moreover, we have well-tested and efficient python code to execute the modelling workflow.

Upon the completion of a computational model of active deformable particles, study into the movement of the system can be explored. As 1B demonstrates, cells can adapt to fit through different geometries. Similarly, this should be tested and replicated with our computational model. Research into how dense systems of active deformable particles behave can also be done with our model. This would be particularly beneficial for samples such as the micro-graph of oligodendroglioma 1A.

Taken together, we have built a powerful model and modelling software that will eventually give profound insights into a range of biological cell behaviour and inform design principles for artificial technology based on active matter.

- 
- [1] M. Abercrombie, “The croonian lecture, 1978 - the crawling movement of metazoan cells,” *Proceedings of the Royal Society of London. Series B. Biological Sciences* **207**, 129–147 (1980).
  - [2] A. Mogilner and B. Rubinstein, “The physics of filopodial protrusion,” *Biophysical Journal* **89**, 782–795 (2005).
  - [3] M. C. Marchetti, J. F. Joanny, S. Ramaswamy, T. B. Liverpool, J. Prost, Madan Rao, and R. Aditi Simha, “Hydrodynamics of soft active matter,” *Reviews of Modern Physics* **85**, 1143–1189 (2013).
  - [4] M. Lisa Manning, “Essay: Collections of deformable particles present exciting challenges for soft matter and biological physics,” *Physical Review Letters* **130** (2023), 10.1103/physrevlett.130.130002.
  - [5] David B. Brückner, Matthew Schmitt, Alexandra Fink, Georg Ladurner, Johannes Flommersfeld, Nicolas Arlt, Edouard Hannezo, Joachim O. Rädler, and Chase P. Broedersz, “Geometry adaptation of protrusion and polarity dynamics in confined cell migration,” *Physical Review X* **12** (2022), 10.1103/physrevx.12.031041.